# Cone Contributions to Cat Retinal Ganglion Cell Receptive Fields

RICHARD A. CROCKER, JAMES RINGO, MYRON L. WOLBARSHT, and HENRY G. WAGNER

From the Department of Ophthalmology, Duke University Medical Center, Durham, North Carolina 27710, and the Laboratory of Neurophysiology, National Institute of Neurological and Communicative Diseases and Stroke, Bethesda, Maryland 20014

ABSTRACT Extracellular microelectrode recordings were made from ganglion cells of the intact, *in situ* eyes of adult common domestic cats. Three different photopic systems, with peak spectral sensitivities at 450, 500, and 556 nm, were observed. All ganglion cells received input from a cone system with a peak spectral sensitivity of 556 nm. The blue-sensitive cone system was observed in about one-half of the ganglion cells studied. In each case the 450-nm cone system contributed to only one functional type of response, either ON or OFF, in the same cell. The other two photopic systems most often contributed to both the ON and OFF responses of an individual ganglion cell. In four cases the 450-nm cone system mediated responses that were opponent to those of the other two photopic systems. The third photopic mechanism has a peak spectral sensitivity at 500 nm and contributed to most receptive field surrounds and many receptive field centers. It is distinguished from the rod system by the occurrence of a break in both dark-adaptation curves and increment-sensitivity curves. No apparent differences in receptive field cone contributions between brisk-sustained and brisk-transient cells were seen.

## INTRODUCTION

The early electrophysiological analysis of the cat retina by Granit (1943 and 1948) and his co-workers suggested that there is more than one cone type. Under scotopic conditions, they observed good agreement between the spectral-sensitivity curves of many cat retinal ganglion cells and visual purple data. However, with other ganglion cells, especially under photopic conditions, the curves showed "humps," often at the blue end of the spectrum, but frequently also at the red end. By direct and indirect means they sought to separate the very broad and irregular dominator curves into narrow modulator curves with single peaks. They found so many maximums that the spectral sensitivities of the primary photochemical substances were not clear. They proposed that the various phenomena could be grouped into three regions of the spectrum, and that there were three chromatically distinct cone populations.

Until recently, attempts to demonstrate by behavioral tests the existence of

J. GEN. PHYSIOL. © The Rockefeller University Press · 0022-1295/80/12/0763/23 $1.00 763
Volume 76 December 1980 763–785

wavelength discrimination in the cat have led to negative results or, at most, to positive results that were very difficult to obtain. The work of Gunter (1954) and of Meyer et al. (1954) failed to show any wavelength discrimination in the cat. Sechzer and Brown (1964) succeeded in training cats to distinguish between broad-band green and red lights. Other behavioral studies confirmed that the cat can be trained, although with great difficulty, to distinguish long from short wavelengths (see, e.g., Mellow and Peterson [1964] and Meyer and Anderson [1965]). Daw and Pearlman (1969) examined the wavelength sensitivity of the cat in extracellular recordings from single units in the lateral geniculate and in the optic tract. At background levels exceeding rod saturation according to their tests, they found evidence for only one cone mechanism (556-nm peak sensitivity). They followed these electrophysiological studies with a series of psychophysical tests (Daw and Pearlman, 1970) and were able to demonstrate that cats can discriminate wavelengths at mesopic levels. This was at first thought to be the behavioral correlate to the rod-cone interaction observed in single-unit recordings. However, because their psychophysical data indicated that cats retained wavelength-discrimination ability at photopic levels, they reexamined lateral geniculate single-unit responses (Pearlman and Daw, 1970; Daw and Pearlman, 1970) and were able to identify a blue cone mechanism. In four of the 434 units studied they found the input of a 445-nm cone system. Each unit had an ON response to blue light and an OFF response to yellow light in the receptive field center. Cleland and Levick (1974 *b*) reported that they occasionally found retinal ganglion cells in the cat that responded preferentially to blue light at photopic levels. This reaffirmed the existence of a second cone mechanism in the cat.

A partial explanation of the difficulty in training cats to make wavelength discrimination has been furnished by Loop and Bruce (1978), who showed that cats very quickly and easily learn wavelength-discrimination tasks when stimulus spots were large. They concluded that the difficulties encountered in earlier behavioral testing resulted from the use of small stimulus spots. The results of Loop and Bruce's behavioral experiments agree with earlier work in suggesting that the cat is a dichromat. However, only broad-band chromatic stimulus test spots have been used to study the cat's behavior. The importance of using highly saturated chromatic light to distinguish dichromacy from a (weak) form of trichromacy has been shown by Jacobs (1977) in his work on the owl monkey, another supposed dichromat. Thus, the results of the behavioral experiments to date do not exclude the possibility that the cat has weak trichromatic vision at photopic levels.

The present study was designed to investigate the wavelength-discriminating mechanisms at the level of the retinal ganglion cell in the cat and, in particular, to investigate the contribution of the blue cone system to the ganglion cells of the retina by using restricted spatial stimulus spots and the intense chromatic adaptation levels made available with a Maxwellian view optical system.

## METHODS

Extracellular ganglion cell recordings were obtained from the intact eyes of adult common domestic cats. Ether was used to induce and to maintain anesthesia for the

duration of surgery. In addition, subcutaneous injections of local anesthetic were made at incision sites before surgery. The animals were paralyzed with an initial intravenous dose of 20 mg of gallamine triethiodide (Flaxedil, American Cyanamide Co., Pearl River, N. Y.). They were maintained on a continuous intravenous infusion of a gallamine and tubocurarine chloride mixture in saline adjusted to provide ~20 mg of gallamine and 0.75 mg of tubocurarine per hour per kilogram weight of the cat. When spontaneous breathing ceased, the animals were artificially respired with a humidified mixture of 30% oxygen and 70% nitrous oxide. End tidal carbon dioxide concentration was maintained at ~4%. Body temperature was maintained at ~37°C. Heart rate and electroencephalogram wave form were observed throughout the experiments.

### *Optical Stimulation*

Optical stimulation was provided by a Maxwellian view system adapted from a two-channel system similar to that described by Wagner et al. (1960). Interference filters were substituted for the monochromator that was a part of the earlier system. 13 two-cavity, narrow band-pass filters (Ditric Optics, Inc., Marlboro, Mass.) with transmission peaks in 20-nm steps from 420 to 660 nm were used. All had 3–7 nm bandwidths at half-maximum amplitude and peak transmission of 45–60%. The filters were mounted on a disk that could be rotated through the collimated region of one channel. Broad-band gelatin filters (Wratten-type, Eastman Kodak Co., Rochester, N. Y.), as listed in Table I, were placed in the other channel and used for chromatic adapting light. The beams of the two channels were combined and positioned so that they passed through a flat-faced contact lens at the center of the fully dilated pupil and formed a focused, demagnified (10:1) image of the apertures on the retina. Each of the coextensive beams covered 20° on the retina. The beam was 5 mm in diameter at the cornea, so no artificial pupil was needed.

The optical system output energy was determined with a thermopile (Epply Laboratory, Inc., Newport, R. I.) which was calibrated by a standard lamp (Epply-type NALCO A-10), whose calibration is traceable to the National Bureau of Standards. In all the figures, 0.0 log units on the sensitivity scale is $1.75 \times 10^{11}$ photons $deg^{-2}$ $s^{-1}$ at the cornea.

### *Electrophysiological Recording*

Metal electrodes of the type described by Levick (1972) were used for ganglion cell recordings. They were backed into a plastic carrier, fitted into a trochar assembly, and attached to a hydraulic drive. The signal was processed by conventional amplification and display systems.

### *Experimental Protocol*

After the electrode had been inserted in the eye and attached to the supporting base plate, the stimulus beam was adjusted to illuminate the selected retinal area, (usually the area centralis) while passing through a flat-faced contact lens at the approximate center of the dilated pupil. The area centralis was identified by the characteristic pattern of the surrounding retinal vasculature and often by a dark-green pigmentation in the otherwise greenish-yellow tapetum (Bishop et al., 1962). Focus was achieved by projecting a fine grid onto the retina and moving the animal to maximize contrast of the grid image. The high reflectivity of the tapetum of the cat eye made this very easy. The electrode drive was assembled and the electrode was hydraulically advanced

under visual observation to a point, close to the retina, in the approximate center of the stimulus beam. The main stimulus beam of unfiltered, tungsten light ("white" light) was then flashed repeatedly and the electrode advanced very slowly until the response of a single ganglion cell was isolated.

A yellow filter was then inserted in the alternate optical channel for background adaptations (Wratten No. 15 attenuated 2 log units; see Table I for filter characteristics). The main stimulus beam was reduced to a small spot of white light, flashed at 0.5 Hz and projected systematically on various areas of the retina to determine the cell's receptive field. The receptive field is the locus of all retinal points that respond to a stimulus. The center was defined as that region that responded with the same stimulus phase (ON or OFF, but not both) as the most sensitive area of the receptive field. Generally, a 0.5° spot was used, but if the receptive field center measured with this spot was <1° the plot was repeated with a 0.2° spot. In our series of experiments, center sizes varied from 0.4 to 5.0°. All but a few cells were concentrically organized center-surround cells as described by Kuffler (1953).

TABLE I

WRATTEN FILTER CHARACTERISTICS

| Wratten filter No. | Effective band pass | 0.0 log units attenuation of irradiance at the cornea | 0.0 log units attenuation in rod-equivalent quanta of 500-nm light at the cornea |
|---|---|---|---|
| | *nm* | $\mu W\ cm^{-2}$ | *photons* $deg^{-2}\ s^{-1}$ |
| 15 | 520–660* | 650 | $1.5 \times 10^{12}$ |
| 21 | 550–660* | 426 | $0.7 \times 10^{12}$ |
| 30 | 410–470‡ | 20 | $0.6 \times 10^{12}$ |
| | 570–660* | 400 | |
| 47A | 470–520 | 70 | $0.7 \times 10^{12}$ |

* 660 nm is an arbitrarily chosen cutoff point in the calculations of transmitted photon flux. These Wratten filters transmit well beyond 660 nm, but that light has a negligible effect on cat photoreceptors.

‡ The lower limit of 410 nm is imposed by the light source used, not by the Wratten filter.

The cell was then classified as sustained or transient on the basis of the standing contrast test described by Cleland et al. (1973) and Cleland and Levick (1974 *a*).

For an ON center cell a spot of white light about one-half the diameter of the center was placed in the middle of the cell's receptive field center. For an OFF center cell the white light in the full-field stimulus channel (20°) was left on and a small dark spot of a diameter slightly larger than the center was rapidly (~0.1) brought from entirely outside the stimulus beam to a position blocking the light in the stimulus beam from reaching the center of the cell's receptive field. These tests were performed against the same background as that used to plot the receptive fields. The intensity of the stimulus light was set 1 log unit above the minimum intensity at which a response to the test could be discerned by ear. The stimulus, dark or light spot, was left in place for 20 s, and the response before, during, and after this stimulus was recorded and examined. Vigorously responding cells showing inhibition at the termination of the sustained stimulus were classified as brisk; brisk sustained if they exhibited a sustained response for the stimulus duration; brisk transient if their response was

phasic, i.e., dropped to the level of maintained activity within 2 s. Cells that did not respond vigorously, that showed no postexcitatory inhibition and that had large receptive fields, a low level of maintained activity, and action potentials made up of low-frequency components were classified as sluggish. No attempt was made to divide the sluggish cells into sustained and transient catagories. For approximately one-third of the cells studied there was some doubt as to the appropriate classification. Those cells were left unclassified.

Threshold spectral-sensitivity curves were then determined by listening to the cell's discharge over a loudspeaker. Thresholds were defined as the least illumination from a square-wave (1 s on and 1 s off) stimulus that produced a discernible increase in firing rate to the onset (ON response) or offset (OFF response) of the stimulus in more than two-thirds of the trials. Thresholds were approached from below, increasing illumination by 0.1-log unit steps until the response criterion was met for six or more flashes.

Threshold and background light values are given in photons per second per square degree (deg) of vision at the cornea. One degree is approximately 225 $\mu$m on the retina for the average adult cat. Sensitivity is defined as the reciprocal of threshold.

The spectral sensitivity curves of the receptive field center were usually taken with an aperture that produced a spot about one-half the center diameter. This size was chosen to minimize any effects of scattered light and isolate the center responses as much as possible, while sufficient "monochromatic" light flux to stimulate the cell was retained. For similar reasons, the surround was usually investigated with an annulus of inner diameter greater than or equal to 1.5 times the receptive field center's diameter, and an outer diameter well within the confines of the 20° diameter background light.

After any change in background light, the cell was adapted, allowing 1 min for each 0.1-log change in intensity for backgrounds of the same chromaticity, and 10 min for any change in chromaticity. Repeat runs showed these times to be sufficient.

We followed the customary practice of describing the photopic processes by the wavelength of maximum absorption expressed in nanometers or by the hue sensation evoked in humans by that wavelength. For example, the cat retinal process, which has a peak sensitivity at 450 nm, is called the 450-nm photopic process (or cone system), or is referred to as the "blue" cone system.

For convenience, we have described the photopic processes recorded at the ganglion cell level as cone systems. However, the morphology of the particular photoreceptor types involved is not known.

## RESULTS

The results will be described on the basis of the individual cone systems inasmuch as these experiments were primarily designed to reveal the cones of the cat retina and investigate their individual properties. The cone interactions now are being investigated and the results will be reported later. The spectral characteristics of 75 ganglion cells are reported here. Most were located in the area centralis or within 10° of it.

### *556-nm Cone System*

The 556-nm cone mechanism furnished the main photopic input to most, if not all ganglion cells. Its appearance in the spectral sensitivity curves could only rarely be completely suppressed with even intense yellow or red adapting light.

In agreement with Daw and Pearlman (1969), we found the spectral curve of the 556-nm cone system slightly narrower than that of the 556-nm Dartnall (1953) nomogram. Fig. 1 shows the spectral sensitivity of the 556-nm cone system in isolation. Its presence can to some degree be seen at the red end of all the spectral sensitivity curves illustrated in this paper.

*450-nm Cone System*

The blue cone system (peak sensitivity at 450 nm), first observed in the cat lateral geniculate nucleus by Daw and Pearlman (1970), contributed to the responses of 38 of the 75 retinal ganglion cells described in this study. Each of the 38 units had an antagonistic center-surround receptive field structure when studied with white light. The blue cone system, however, was not

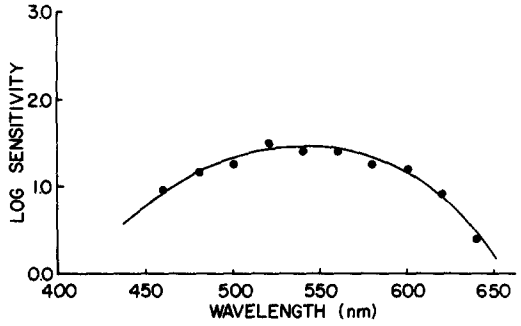


FIGURE 1. The spectral sensitivity of the center of an ON-center, OFF-surround ganglion cell. The center diameter was 1.7°. Center ON responses were examined with a 0.8° spot periodically flashed on for 1 s and off for 1 s in the middle of the cell's receptive field center. Adapting light was provided by a yellow (Wratten No. 15) background, equivalent in its effect on the rod system to $1.5 \times 10^{10}$ photon $deg^{-2}$ $s^{-1}$ of 500-nm light. The continuous curve is taken from Daw and Pearlman (1969) (their Fig. 10) and is the average 556-nm cone curve. This cell is a brisk-transient type, as judged by the criterion discussed in Methods. Zero log units on the sensitivity scale is $1.75 \times 10^{11}$ photon $deg^{-2}$ $s^{-1}$ at the cornea.

observed to have the spatially antagonistic receptive field structure seen in the other cone systems. In 23 of these 38 units the blue cone was excited by the cessation of the light (OFF), and in the remaining 15 units the blue cone was excited by the onset of the light (ON). Fig. 2 shows the spectral-sensitivity curves of a unit in which a blue cone OFF response could be recorded with a small centered spot or a concentric annulus. The spot was well within the cell's receptive field center (as defined in Methods), and the annulus is well outside the center. This is confirmed by the 556-nm cone spectral-sensitivity curves, because for the 556-nm cone system only ON responses were found with the spot stimulus and only OFF responses were found with the annulus. No mixed (ON and OFF) responses were observed. Special care was taken to ensure that the spatial information was accurate. The image quality on the

retina remained very good, and there was no indication of eye movement during the course of the experiments. This cell was atypical in that the blue cone system could be directly measured in both the center and surround. Four such cells were found. All four received ON-center, OFF-surround input from the 556-nm cone system and were ON-center, OFF-surround units when initially plotted with a small spot of white light. Two of these four units received blue cone OFF contributions to both center and surround, while the other two received blue cone ON contributions to both regions.

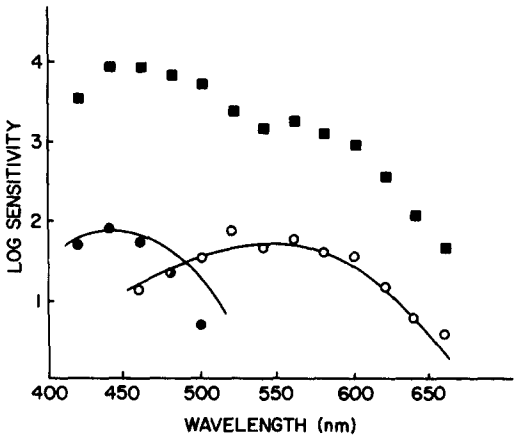


FIGURE 2. The spectral sensitivity of an ON-center, OFF-surround brisk-transient cell (see text for details of the classification scheme) examined with yellow (Wratten No. 15) adapting light. The center diameter was 2°. The center ON responses (○) and OFF responses (●) were examined with a spot approximately 1° in diameter on the retina. The surround OFF responses (■) were examined with an annulus (i.d. 4°, o.d. 15° on the retina). Both the blue cone system and the 556-nm cone system are evident in the surround responses. Center responses are driven by the 556-nm system. Antagonistic, blue cone–mediated OFF responses are also seen in the center region. The yellow (Wratten No. 15) background light was equivalent in its effect on the rod system to $1.5 \times 10^{10}$ photons of 500-nm light $deg^{-2}\ s^{-1}$. Zero log units on the sensitivity scale is $1.75 \times 10^{11}$ photons $deg^{-2}\ s^{-1}$ at the cornea. The solid curve in the short wavelengths is the photopigment absorption curve for a peak at 450 nm derived from the Dartnall (1953) nomogram. The solid curve at the long-wavelength end of the spectrum is the average 556-nm cone curve from Fig. 1.

More commonly (34 of the 38 units with blue cone input), the blue cone could be observed in only one region (center or surround) of the receptive field. In that region the blue cone system responded to the same phase (ON or OFF) as the 556-nm cone system did (Fig. 3). Of these 34 units, 25 had a blue cone contribution to the surround and 9 had blue cone contributions to the center. The units with surround contribution were divided evenly between ON and OFF (12 ON surrounds, 13 OFF surrounds). However, the 9 units with blue cone center contribution were all of the ON-center type. Table II summarizes the 450-nm cone system data.

In a few cases the spatial characteristics of the blue cone mechanism were studied in greater detail. These experiments further established the unusual receptive field properties of the 450-nm cone system. 5 units that showed a 450-nm cone-system input to just one region (center or surround) by the usual spatial analysis were further studied with a series of annuli of various inner

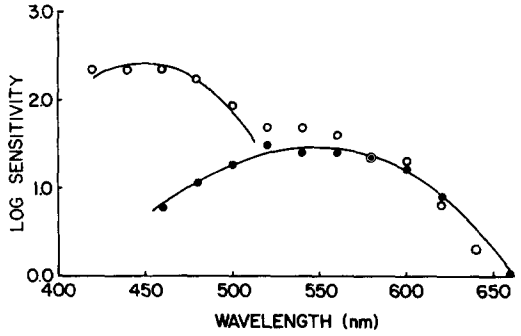


FIGURE 3. The spectral sensitivity of an OFF-center, ON-surround ganglion cell. The center diameter was 3°. The center OFF responses (●) were mediated by the 556-nm cone system, and the surround ON responses (○) showed contributions from both the 450-nm and the 556-nm cone systems. The center was examined with a 1° diameter spot, and the surround was examined with a 5° i.d., 15° o.d. annulus. Stimulation was 0.5-Hz square wave. The adapting light was yellow (Wratten No. 15) for examining both the center and the surround. This cell responded briskly but could not be classified as sustained or transient by the criterion discussed in the text. The yellow (Wratten No. 15) background light was approximately equivalent in its effect on the rod system to $1.5 \times 10^{10}$ photons $deg^{-2}$ $s^{-1}$ of 500-nm light for center examination and $5 \times 10^{10}$ photons $deg^{-2}$ $s^{-1}$ of 500-nm light for surround examination. The solid curves are the same as in Fig. 2. Zero log units on the sensitivity scale is $1.75 \times 10^{11}$ photons $deg^{-2}$ $s^{-1}$ at the cornea.

TABLE II

RESPONSES OF THE 450-nm CONE SYSTEM

| | Brisk sustained | | | Brisk transient | | | Unclassified | | |
|---|---|---|---|---|---|---|---|---|---|
| 555-nm cone responses | Location | Response type | Number found | Location | Response type | Number found | Location | Response type | Number found |
| Center ON/ surround OFF | Center only | ON | 6 | Center only | ON | 0 | Center only | ON | 3 |
| | Surround only | OFF | 2 | Surround only | OFF | 5 | Surround only | OFF | 6 |
| | Both center and surround | ON | 2 | Both center and surround | ON | 2 | | | |
| Center OFF/ surround ON | Center only | OFF | 0 | Center only | OFF | 0 | Center only | OFF | 0 |
| | Surround only | ON | 3 | Surround only | ON | 3 | Surround only | ON | 6 |

No 450-nm cone input was seen in the four sluggish units recorded.

and outer diameters. The direction (ON response or OFF response) of the blue cone-system input remained unchanged across the region where the direction of the other cone systems reversed, the center-surround boundary as determined with white light stimulation (Fig. 4). In two of these units the

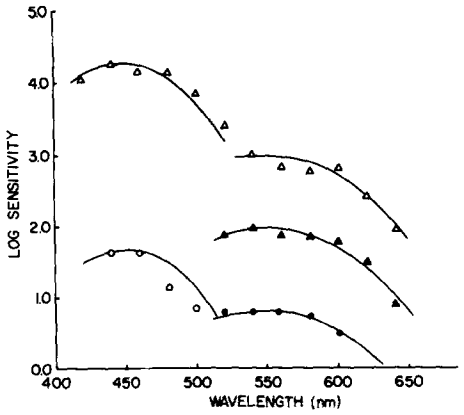


FIGURE 4. The spectral sensitivity of an OFF-center, ON-surround ganglion cell. The center diameter was 2.5°. The solid curved lines in the short wavelengths are from the Dartnall (1953) nomogram for a 450-nm peak. The solid curves in the long wavelengths are the 556-nm cone curve from Fig. 1. These curves have been adjusted up and down to provide a good fit by eye. All responses were examined with 0.5-Hz square-wave stimulus and under adaptation by an orange (Wratten No. 21) background. The center (▲) was examined with a 1° diameter spot, and the surround (△) was examined with a 3.5° i.d., 12 degree o.d. annulus. The center responses (▲), translated up 1 log unit for clarity, were mediated by the 556-nm cone. As a result of limitation in stimulus intensity, no responses were found for short-wavelength stimulation. That is as would be expected for the 556-nm cone at the sensitivity level shown (e.g., the 556-nm cone curve [Fig. 1] predicts that the threshold for the 556-nm cone should be ~0.5 log units higher for stimulation with 460-nm light than with 560-nm light. In this case that would mean a threshold with 460-nm light stimulation of $5.0 \times 10^{10}$ photons $deg^{-2}$ $s^{-1}$. Our apparatus was able to deliver only $2.0 \times 10^{10}$ photons $deg^{-2}$ $s^{-1}$ of 460-nm light). The surround responses (△), translated up 2 log units for clarity, were mediated by the 450-nm and 556-nm cone systems. The spectral sensitivity in a narrow annular region (i.d., 2.0°; o.d., 3.5°) was examined under the same adapting conditions. These responses (●, OFF and ○, ON) show a surround like contribution from the 450-nm cone system and a centerlike contribution from the 556-nm cone system. This cell responded briskly but could not be classified as sustained or transient. The orange (Wratten No. 21) background light was equivalent in its effect on the rod system to $7 \times 10^{11}$ photons $deg^{-2}$ $s^{-1}$. Zero log units on the sensitivity scale is $1.75 \times 10^{11}$ photons $deg^{-2}$ $s^{-1}$ at the cornea.

center-type responses mediated by the 450-nm cone system clearly extended into the surround region, and, in the other three, surround-type responses mediated by the 450-nm cone system extended into the center region.

*500-nm Photopic System*

A third chromatically distinct, photopic process was commonly found to contribute to cat ganglion cell responses. It has a peak spectral sensitivity at ~500 nm (Fig. 5). We believe that this 500-nm process may be a cone rather than a rod because it could be measured against background light levels well into the photopic range, and because its dark-adaptation and increment-sensitivity curves showed breaks similar to typical rod-cone breaks.

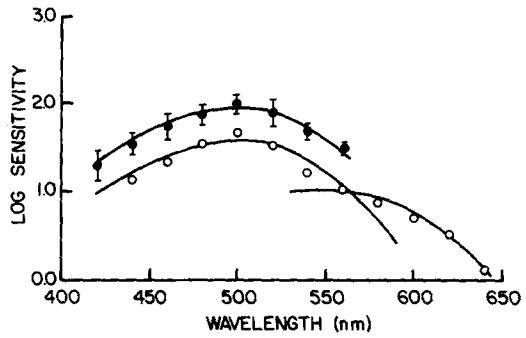


FIGURE 5. Average spectral sensitivities (●) (420 nm through 560 nm) for the first 21 units that showed a 500-nm peaking process under photopic adaptation, equivalent for the rod system to $1.0 \times 10^9$ photons $deg^{-2}$ $s^{-1}$ or more. The error bars represent ±1 SD from average values. Adapting backgrounds were either magenta (Wratten No. 30), when the cell had a contribution from the 450-nm and 556-nm cone systems), or yellow (Wratten No. 15) or orange (Wratten No. 21), when the cell had no contribution from the 450-nm cone system. The general shape and peak value were approximately the same from unit to unit and shifts of the illuminance of the adapting light shifted the sensitivity values up and down the sensitivity axis without changing the general shape of the curve. This indicates that a single process is involved. A good but still typical example is shown by the open circles. This is the surround spectral sensitivity of a brisk-transient cell with a 2.5° diameter center. It was examined with an annulus (i.d., 5°; o.d., 15°) flashed at 0.5 Hz, and adapted with a magenta background (Wratten No. 30), equivalent in its effect on the rods to $6 \times 10^{10}$ photons $deg^{-2}$ $s^{-1}$ of 500-nm light. The continuous curves in the short and middle wavelengths are from the Dartnall (1953) nomogram for a 500-nm peak. The continuous curve in the long wavelengths is the 556-nm cone curve from Fig. 1. Zero log units on the sensitivity scale is $1.75 \times 10^{11}$ photons $deg^{-2}$ $s^{-1}$ at the cornea.

Fig. 6 shows an increment-sensitivity curve, measured for the center mechanism of a cell, demonstrating rod saturation at or before a background equivalent for the rods to $6 \times 10^8$ photons $deg^{-2}$ $s^{-1}$ of 500-nm light. The spectral-sensitivity curves before and after rod saturation are shown in Fig. 7. Clearly, the center mechanism of this cell had no contribution from a 500-nm photopic process, so we were able to chromatically adapt the cones selectively and reveal rod saturation. Our measurements agree well with other reports. Rodieck and Ford (1969) report rod saturation in the electroretinogram at

about $8 \times 10^8$ photons $deg^{-2}$ $s^{-1}$, and Lennie et al. (1976) show complete rod saturation at $\sim 1 \times 10^9$ photons $deg^{-2}$ $s^{-1}$.

The surround mechanism of the cell in Fig. 6 had a clear contribution from a 500-nm process (as shown in Fig. 8) at a background equivalent for the rods to $6 \times 10^9$ photons $deg^{-2}$ $s^{-1}$ at 500 nm. In other cells we could observe contributions from the 500-nm photopic process against very intense magenta backgrounds. For example, in the single-cell data shown in Fig. 5 the background is equivalent for the rod system to $6 \times 10^{10}$ photons $deg^{-2}$ $s^{-1}$ at 500 nm, and in the bottom curve of Figure 13 the background is equivalent for the rod system to $1.2 \times 10^{11}$ photons $deg^{-2}$ $s^{-1}$ at 500 nm. One cell had a

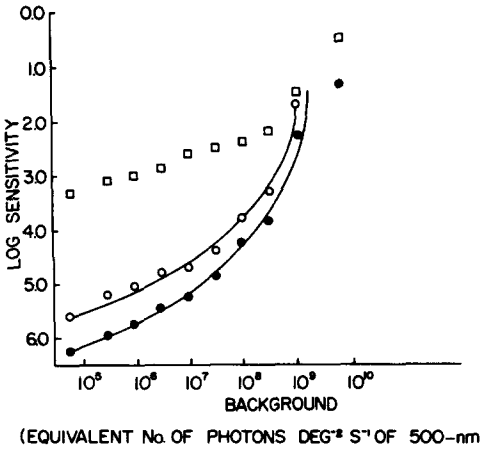


FIGURE 6. Increment-sensitivity curves for the center of a brisk-transient ganglion cell. The center was 1.0° in diameter and was stimulated at 0.5 Hz with a 0.67° diameter spot of 440-nm (○), 500-nm (●), and 640-nm (□) light. Threshold values were determined at each of an increasing series of magenta (Wratten No. 30) adapting background illuminances from one equivalent in its effect on the rod system to $5 \times 10^4$ photons $deg^{-2}$ $s^{-1}$ of 500-nm light to one equivalent to $6 \times 10^9$ photons $deg^{-2}$ $s^{-1}$ of 500-nm light. The two continuous curves follow the rod adaptation (see Fig. 7 for spectral data) and are the same curve translated up and down only. In this figure and in Fig. 10 and 12, sensitivity increases going down the ordinate. Zero log units on the log-sensitivity scale is $1.75 \times 10^{11}$ photons $deg^{-2}$ $s^{-1}$ at the cornea.

strong enough contribution from the 500-nm photopic process that it could be observed against an adapting background of white light (color temperature, 2,950°K), equivalent in its effect on the rod system to $\sim 1.0 \times 10^{11}$ photons $deg^{-2}$ $s^{-1}$ at 500 nm (Fig. 9).

Fig. 10 shows the increment threshold curves for a cell that did have a 500-nm photopic process contributing to the region (surround in this case) in which the increment thresholds were measured. Here the rod saturation is not as obvious as in Fig. 6 because selective chromatic adaptation was not possible (the rod and the 500-nm photopic process have very similar or identical spectral sensitivities). Nevertheless, a saturation is clearly occurring at or near

a background equivalent for the rod to $6 \times 10^8$ photons $deg^{-2}$ $s^{-1}$ at 500 nm. The spectral-sensitivity curves before and after saturation are shown in Fig. 11, and the 500-nm photopic process is evident against the background equivalent for the rods to $6 \times 10^{10}$ photons $deg^{-2}$ $s^{-1}$ at 500 nm, 2 log units above rod saturation.

To confirm that this response was a photopic process we followed the dark adaptation time-course of the centers of three ganglion cells and the surround

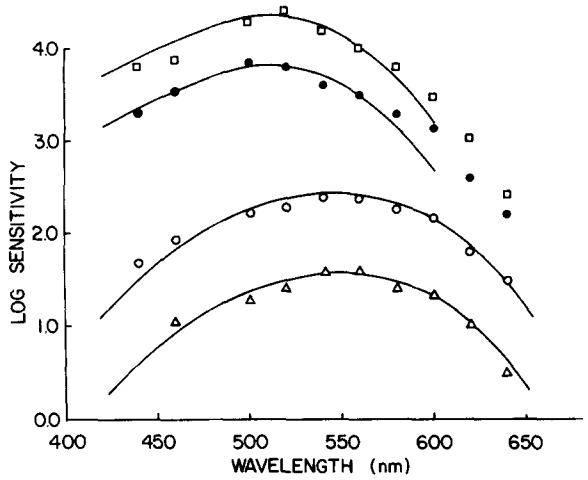


FIGURE 7. Same unit as in Fig. 6. The spectral sensitivities of the ON response in the center, taken at 0.5 Hz with a 0.67° spot during the increment-sensitivity series. The magenta (Wratten No. 30) adapting background was equivalent in its effect on the rod system to $1 \times 10^8$ (□), $3 \times 10^8$ (●), $1 \times 10^9$ (○), and $6 \times 10^9$ (△) photons $deg^{-2}$ $s^{-1}$ of 500-nm light. The continuous curve through the upper two sets of points is the Dartnall (1953) nomogram for the cat rod (507-nm peak). The continuous curve through the lower two sets of points is the 556-nm cone curve. The rod system's influence is prominent in the curve taken against a background of Wratten No. 30 equivalent to $1 \times 10^8$ and $3 \times 10^8$ photons $deg^{-2}$ $s^{-1}$ but has disappeared for the backgrounds equivalent to $1 \times 10^9$ and $6 \times 10^9$ photons $deg^{-2}$ $s^{-1}$ of 500-nm light. This Purkinje shift between background equivalent to $3 \times 10^8$ and $1 \times 10^9$ photons $deg^{-2}$ $s^{-1}$ agrees with the rod saturation point of $\sim 6 \times 10^8$ photons $deg^{-2}$ $s^{-1}$ of 500-nm light from Fig. 6. Zero log units on the log-sensitivity scale is $1.75 \times 10^{11}$ photons $deg^{-2}$ $s^{-1}$ at the cornea.

of four others in which the 500-nm photopic process appeared. In each case the sensitivity increased rapidly to a plateau after the adapting light was turned off, remained at the plateau for a few minutes, then showed a further rapid increase after 20–40 min in the dark (Fig. 12). Throughout the entire recovery, the spectral sensitivity of the ganglion cell responses remained consistent with that of a process with a peak sensitivity for 500 nm (Fig. 13). The threshold sensitivities (measured at the cornea) at the occurrence of the break varied from $1.5 \times 10^6$ to $1 \times 10^7$ quanta of 500-nm light $deg^{-2}$ $s^{-1}$.

The 500-nm photopic process was seen in the receptive field surrounds of 65 of the 75 ganglion cells studied and in the centers of 37 of those 75 units. The 500-nm photopic process appeared with the 556-nm cone system and evoked responses of the same type (ON or OFF) evoked by the 556-nm cone system. No clear antagonism between the two processes was ever observed. The spatial distributions of the two processes within a receptive field region were similar but not always identical.

*Ganglion Cell Classification and Cone Inputs*

Brisk-sustained units, brisk-transient units, and the group of unclassified units (all of which were brisk but not clearly sustained or transient) were similar in

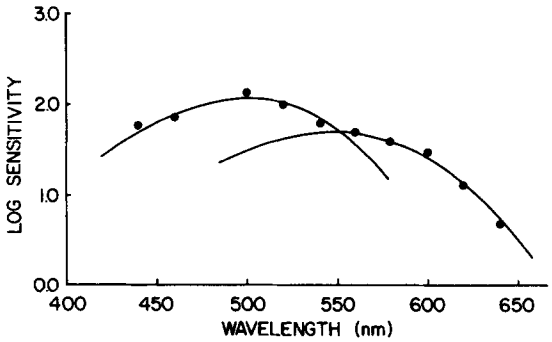


FIGURE 8. The spectral sensitivity of the OFF response of the surround of the unit shown in Fig. 6 and 7. The surround (●) was examined with an annulus (i.d., 1.67°; o.d., 6.0°) flashed at 0.5 Hz. The magenta (Wratten No. 30) adapting background was equivalent in its effect on the rod system to $6 \times 10^9$ photons $deg^{-2}$ $s^{-1}$ of 500-nm light. This was the same background as was used for center stimulation to obtain the lowest set of data points (△) in Fig. 7. This figure shows the 500-nm photopic process measured in the surround against a background 1 log unit more intense than that which saturated the rod system of the center. The continuous curve in the short and middle wavelengths is the Dartnall (1953) nomogram for a process peaking at 500 nm. The continuous curve in the long wavelengths is the 556-nm cone curve. Zero log units on the log-sensitivity scale is $1.75 \times 10^{11}$ photons $deg^{-2}$ $s^{-1}$ at the cornea.

their cone-system inputs. Only four sluggishly responding units were studied and none of these had a 450-nm cone-system input. Each had a strong 556-nm cone-system input, and three of the four units had an input from the 500-nm photopic system.

## DISCUSSION

In this study we found the blue cone system to be a frequent contributor to ganglion cell receptive fields. We could distinguish a 450-nm cone-system contribution to about one-half of the cells examined, whereas other workers have reported blue cone contributions to be rare. Daw and Pearlman (1970) examined 434 lateral geniculate units and found only four with blue cone

input, and Cleland and Levick (1974 *b*) found six such cells out of 73. Each of those units had spectrally opponent centers with 450-nm cone-mediated ON responses and 556-nm cone-mediated OFF responses. In these studies all of the units with a blue cone contribution were color opponent. The high frequency of blue cone contributions that we found, as opposed to the rarity of such contributions in previous studies, may be due to our detection of nonopponent blue cone contributions (34 nonopponent units of 38 units with blue cone contributions) or to the higher stimulus intensities available to us from our Maxwellian view arrangement.

In the present study four opponent cells were observed. The cone input to these cells is diagrammed in Fig. 14. An important characteristic of all four cells is that the 450-nm cone is opponent to the 556-nm cone in one region of the receptive field and is nonopponent in the other region.

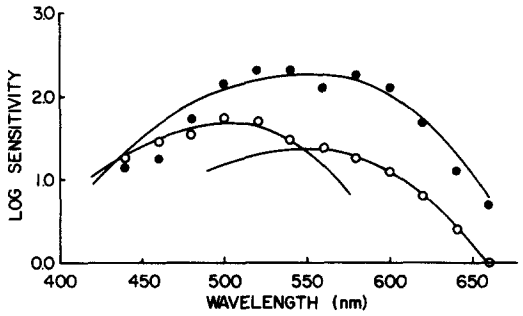


FIGURE 9. The spectral sensitivities of a brisk-sustained, OFF-center/ON-surround unit. The center (●) was examined with a 1.0° diameter spot (center diameter, 1.5°) flashed at 1.0 Hz under adaptation from a white (color temperature, 2950°K) background equivalent in its effect on the rod system to ~1.0 × $10^{10}$ photons $deg^{-2}$ $s^{-1}$ of 500-nm light. The surround (○) was examined with an annulus (i.d., 3°; o.d., 17°) flashed at 1.0 Hz under adaptation from a white background equivalent in its effect on the rod system to ~1.0 × $10^{11}$ photons $deg^{-2}$ $s^{-1}$ of 500-nm light. At this background level the surround responses are mediated by the 500-nm photopic process as well as by the 556-nm cone, whereas against a background 1.0 log units lower the center shows no 500-nm process. The continuous curves in the long wavelengths are both the 556-nm cone curve taken from Fig. 1. The continuous curve in the shorter wavelengths is the Dartnall (1953) nomogram for a 500-peak. Zero log units on the log-sensitivity scale is 1.75 × $10^{11}$ photons $deg^{-2}$ $s^{-1}$.

The receptive field characteristics of the blue cone system suggest that the few cells with 450-nm cone-system opponency in the center or surround are just special cases of the usual organization of the ganglion cell receptive field, with an additional blue cone input. Most often the blue cone system appears to be restricted to either the center or the surround of the ganglion cell receptive field. It mediates responses of the same type (ON or OFF) as the other photopic systems contributing to that region. When units of this sort are examined carefully, however, the blue cone system is seen to extend beyond

the center-surround border, without changing response type (ON or OFF), to give a narrow, annular region of opponent responses. The four opponent units discussed above differ from this more common blue cone-system distribution only in having more extensive overlap of the blue cone system across the center-surround border.

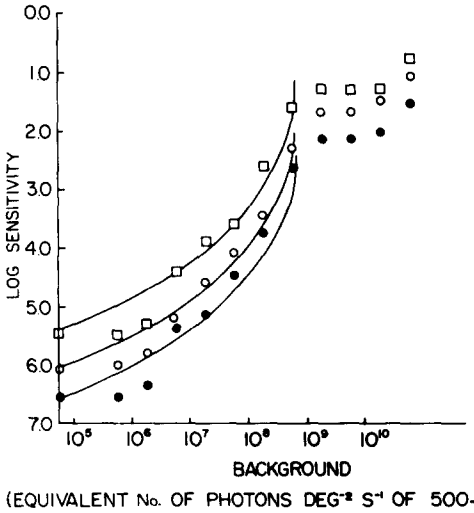


FIGURE 10. Increment-sensitivity curves for the surround of a brisk-transient OFF-center/ON-surround unit. The center diameter was 1.7°. The surround was examined with an annulus (i.d., 2.4°; o.d., 8°) flashed at 0.5 Hz of 500-nm (●), 560-nm (○), and 440-nm (□) light (440-nm data points have been shifted up 0.5 log units on the log-sensitivity axis for clarity). Threshold values were determined at each of an increasing series of magenta (Wratten No. 30) adapting background illuminances from one equivalent in its effect on the rod system to $6 \times 10^4$ photons deg$^{-2}$ s$^{-1}$ of 500-nm light to one equivalent in its effect on the rod system to $6 \times 10^{10}$ photons deg$^{-2}$ s$^{-1}$ of 500-nm light. The continuous curves that follow the rod adaptation are taken from the rod-saturation curve of Fig. 6, and the three curves are shifted up and down on the sensitivity axis only. The large decreases in sensitivity between background intensities equivalent to $10^8$ and $10^9$ photons deg$^{-2}$ s$^{-1}$ indicate that saturation is occurring, and the very small decreases in sensitivity between backgrounds equivalent to $10^9$ and $10^{10}$ photons deg$^{-2}$ s$^{-1}$ show that a new process has taken over. The spectral sensitivities before and after this shift are shown in Fig. 11. In this figure sensitivity increases going down the ordinate. Zero log units on the log-sensitivity axis is $1.75 \times 10^{11}$ photons deg$^{-2}$ s$^{-1}$ at the cornea.

Differences in the receptive field distributions of the blue cone system and the 556-nm cone system were also seen by Cleland and Levick (1974 *b*) in the few blue-sensitive cat retinal ganglion cells they observed.

The organization of the 450-nm cone system in the cat resembles that of the blue cone mechanism described in optic nerve recordings from the ground

squirrel (Michael, 1968; Gur and Purple, 1978). In that animal, spatial antagonism is seen in the long-wavelength cone system but not in the blue system. Michael's class II units in particular are close to those seen in the cat. DeMonasterio and Gouras (1975) described no unusual blue cone receptive field characteristics in the rhesus monkey retina. However, they illustrate (in their Fig. 7) the responses of one concentrically organized cell that apparently

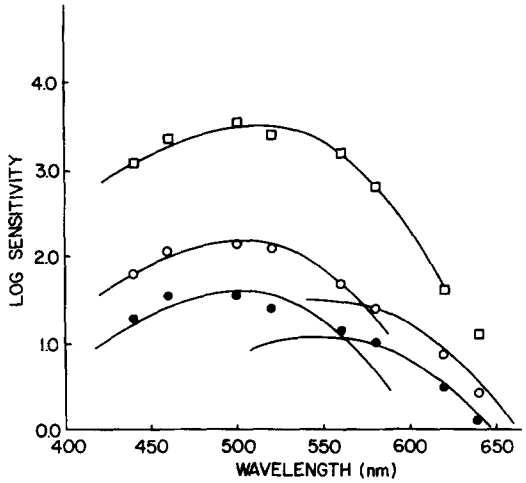


FIGURE 11. The spectral sensitivities of the surround for the unit shown in Fig. 10. The surround responses were examined during the increment-threshold series with an annulus (i.d., 2.4°; o.d., 8°) flashed at 0.5 Hz and against a magenta (Wratten No. 30) adapting background equivalent in its effect on the rod system to $6 \times 10^6$ (□), $2 \times 10^9$ (○), and $6 \times 10^{10}$ (●) photons $deg^{-2}$ $s^{-1}$ at 500-nm light. The data for the background equivalent to $6 \times 10^6$ photons $deg^{-2}$ $s^{-1}$ has been shifted down 2 log units. The continuous curve through the data points for the $6 \times 10^6$ photons $deg^{-2}$ $s^{-1}$ background (□) is derived from the Dartnall (1953) nomogram for a 507-nm peak (the cat's rod curve). The continuous curves in the short wavelengths for the data taken at $2 \times 10^9$ and $6 \times 10^{10}$ photons $deg^{-2}$ $s^{-1}$ background (○ and ●) are derived from the Dartnall nomogram for a 500-nm peak, and the continuous curves in the long wavelengths are the 556-nm cone curve. The relative spectral sensitivities in the short and middle wavelengths are about the same before and after rod saturation (Fig. 10), indicating that the 500-nm peaking process in the lower two curves is a photopic process. Zero log units on the log sensitivity scale is $1.75 \times 10^{11}$ photons $deg^{-2}$ $s^{-1}$ at the cornea, except for the points taken with a $6 \times 10^6$ photons $deg^{-2}$ $s^{-1}$ background, which on this scale would be shifted up 2 log units.

had a blue ON response in both center and surround. The blue cone organization of that cell appears to be similar to that of some cells seen in the cat.

A cat photopic process with rodlike spectral sensitivity was first reported in preliminary descriptions of part of this work (Crocker et al., 1977; Ringo et al., 1977). A similar mechanism has apparently been observed in the ground

squirrel (Tong, 1977) and in the albino rat (Cicerone, 1976). The photopic conditions under which these processes were observed suggest that the photoreceptors involved are different from ordinary rods and may be cones, at least from a functional standpoint. In the cat, this interpretation is supported by the shape of the dark-adaptation curve of the isolated 500-nm photopic process (Fig. 12), which resembles the cone system–recovery curves derived from both behavioral and electrophysiological experiments in other species.

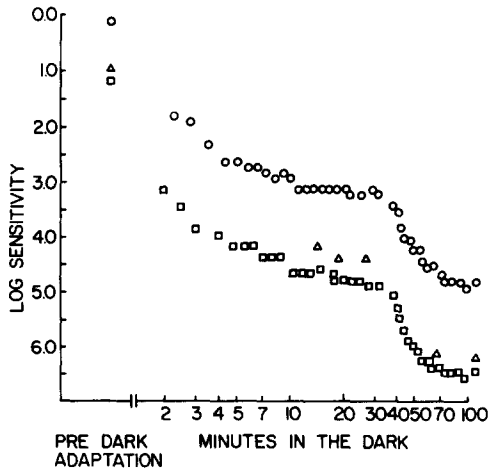


FIGURE 12. The dark-adaptation time-course of the ON-surround responses of a concentric, sluggish unit. The spectral sensitivity of this unit is given in Fig. 13. The circles represent the sensitivity to 620-nm stimulus light, the triangles the sensitivity to 460-nm light, and the squares the sensitivity to 500-nm light. The sensitivity ratios for the three stimulus wavelengths are appropriate for a process with a peak sensitivity at 500 nm both before and after the rapid change in sensitivity at 35 min. The prior light adaptation was 20 min of a magenta (Wratten No. 30) background equivalent for the rod system to $1.2 \times 10^{11}$ photons $deg^{-2}$ $s^{-1}$ of 500-nm light. The light-adapted sensitivities at the three wavelengths just before the beginning of dark adaptation were: 0.1 log units at 620 nm, 0.96 log units at 460 nm, and 1.2 log units at 500 nm on the sensitivity scale used in this figure, where 0.0 log units is $1.75 \times 10^{11}$ photons $deg^{-2}$ $s^{-1}$ at the cornea. In this figure, sensitivity increases going down the ordinate.

Cat ganglion cells with a light-adapted spectral sensitivity peaking at 500 nm show an initial, very rapid recovery of sensitivity in the dark (2–3 log units in the first 3–5 min) while retaining the same spectral sensitivity. After a plateau in the recovery curve, another rapid increase in sensitivity (1–2 log units) occurs after 20–40 min. This puts a kink in the middle of the recovery curve and divides it into two distinct phases. During the second phase the peak spectral sensitivity remains at or near 500 nm, and the sign of the ganglion cell response is unchanged. In numerous human psychophysical experiments (e.g., see Hecht [1937]) and in many studies at the single-unit

level in a variety of species (e.g., see Barlow et al. [1957] and Donner and Rushton [1959]) the kink in dark-adaptation curves has been shown to correspond to a change from cone-to-rod–mediated responses. Typically, in the first phase of dark adaptation, photopic spectral sensitivity persists and colored test lights appear colored. In the second phase, spectral sensitivity follows a scotopic curve and colored test lights are seen as colorless. The kinks in sensitivity-recovery curves of the photopic 500-nm process isolated in cat ganglion cell responses resemble cone-rod breaks. It seems very likely that they too are the result of a shift from cone-to-rod–mediated responses, although no change in spectral sensitivity accompanies the breaks.

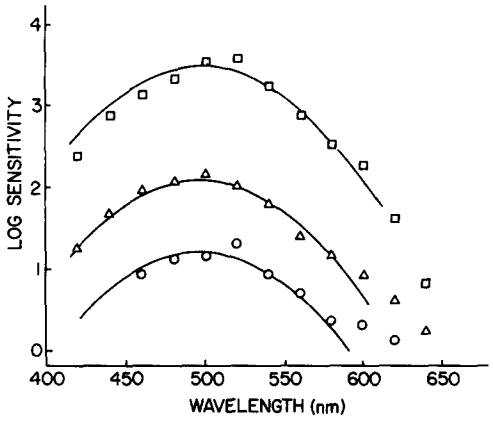


FIGURE 13. The light-adapted and the dark-adapted spectral-sensitivity curves of the ON surround of a concentric, sluggish unit (the same unit shown in Fig. 12). The stimulus was an annulus (i.d., 7°; o.d. 15°) on the retina. ON responses with magenta (Wratten No. 30) adaptation equivalent for the rod system to 2 × $10^{10}$ photons $deg^{-2}$ $s^{-1}$ of 500-nm light (△) show input from the 500-nm photopic system and a much weaker input from the 556-nm cone system. The spectral-sensitivity curve is unchanged at an even higher background level (○, Wratten No. 30 illumination equivalent for the rods to 1.2 × $10^{11}$ photons $deg^{-2}$ $s^{-1}$ of 500-nm light. The dark-adapted spectral sensitivity is shown (□) after more than 100 min in the dark (the data has been shifted down by 3 log units). The time-course of the dark adaptation is in Fig. 12. The continuous curves represent the sensitivity of a single photopigment with a peak sensitivity of 500 nm derived from the Dartnall (1953) nomogram. Zero log units on the sensitivity scale is 1.75 × $10^{11}$ photons $deg^{-2}$ $s^{-1}$ at the cornea.

Further support for the interpretation that the 500-nm photopic process is a cone comes from the increment-sensitivity data. This is shown most clearly in Fig. 10, where it can be seen that under increasing background illumination the cell follows a typical rod increment–sensitivity curve until, in the midst of the saturation segment, the cell abruptly stops decreasing in sensitivity with increases in background illumination. At this point the cell maintains its sensitivity through an increase in background illumination of more than a factor of ten. Throughout the increment-sensitivity measurements the cell

maintains the spectral sensitivity of a 500-nm process. This increment-sensitivity curve is very like an increment-sensitivity curve with changeover from rod to cone and is very unlike any exclusively rod curve we are familiar with.

The existence of a photopic system with peak sensitivity at 500 nm provides a basis for reinterpretation of some previously puzzling data. Bonaventure (1962 and 1964) was unable to demonstrate a Purkinje shift by behavioral tests in the cat. This could have been due to some feature favoring the 500-nm photopic system in his measurement of the photopic spectral sensitivity. LaMotte and Brown (1970), using behavioral methods, measured the photopic sensitivity during the cone plateau of dark adaptation. The resultant spectral-sensitivity curve shows a maximum at 564 nm and a secondary peak at 523 nm. This double-peaked spectral curve is probably caused by a combination

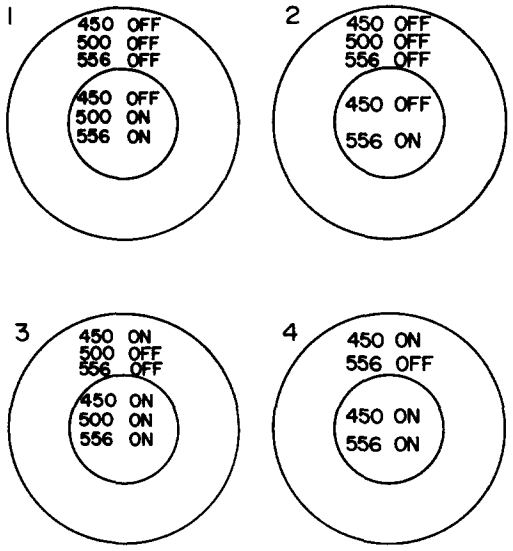


FIGURE 14. Cone contributions to the four spectrally opponent cells. Cells 1 and 2 were brisk transient, cells 3 and 4 were brisk sustained.

of two photopic processes; the obvious candidates are the 500-nm and 556-nm peaking cone systems. Other work on spectral sensitivity, both psychophysical (Gunter, 1954) and electrophysiological (Granit, 1943 and 1948), can also be more clearly interpreted on this basis.

In agreement with previous observations (Daw and Pearlman, 1970), the long-wavelength sensitivity of the common 556-nm cone system was observed to fall off more rapidly than predicted by the Dartnall (1953) nomogram. Such a narrowing of the spectral-response curves mediated by photopigments with peaks at long wavelengths is predicted by a model based on intensity sharirg between the $\alpha$ and $\beta$ absorption bands of the photopigments (Wolbarsht and Yamanashi, 1975 and 1977).

The abundance of the input from three cone systems that we found stands in sharp contrast to previously reported results. Daw and Pearlman's 1970 findings come closest to ours, but there are great differences. Daw and Pearlman did not find a 500-nm photopic system input and found the 450-nm one only very rarely.

The findings of Daw and Pearlman (1970) can be reconciled with the present results by examining the main differences between the two approaches. Daw and Pearlman recorded in the lateral geniculate nucleus, but we feel this is not the source of the difference because we found abundant input from all three cones to sustained cells that are reported to project exclusively to the lateral geniculate nucleus (Fukuda and Stone, 1974). A significant difference lies in the light levels used. Daw and Pearlman had $\sim 4 \times 10^{12}$ photons $cm^{-2}$ $s^{-1}$ of monochromatic stimulus light available at the tangent screen.[1] For the purpose of calculations we assume a perfectly diffusing tangent screen and a 6-mm diameter pupil for effective cone stimulation. This is of course much smaller than the dilated pupil actually used by Daw and Pearlman. However, in calculations of light available on the retina for stimulation of cones, any radiation entering more than 3 mm from the center of the pupil may be ignored because of the Stiles-Crawford Effect. The distance of the tangent screen from the eye makes no difference for intensity calculations so long as the retinal image is large in comparison with the diffraction-limited one. For convenience let us assume a 57-cm distance so that 1 cm on the tangent screen subtends 1° on the retina. Then, a 0.28-$cm^2$ pupil 57 cm from the tangent screen will catch a little less than one part in $10^5$ of the light. This gives a maximum retinal illumination of $4 \times 10^7$ photons $deg^{-2}$ $s^{-1}$ for measurement of cone thresholds. This is significantly less than the threshold intensity we needed when strong chromatic backgrounds were used (e.g., in Fig. 8, against a background of Wratten No. 30, the threshold of the 500-nm cone at its most sensitive wavelength is $1.0 \times 10^9$ photons $deg^{-2}$ $s^{-1}$).

Another possible explanation for the discrepancy is that different chromatic backgrounds were used in the two studies. Daw and Pearlman (1969 and 1970) often used a combination of white- and colored-light backgrounds that would not be very selective for any particular cone type. They also tried more saturated backgrounds of blue (Kodak Wratten No. 47) and yellow (No. 12). Using the blue background they found only the 556-nm cone. This is the same result we got with No. 47 and other blue backgrounds. The yellow filter (No. 12) is a long-wavelength pass filter with 10% transmission at 510 nm and is not selective for a 500-nm photopic process. Wratten No. 12 is, however, fairly selective for the 450-nm cone. We did not use a Wratten No. 12 background but we used Wratten No. 15 and No. 21, which are more selective because of their higher cutoff wavelengths (for No. 15 the 10% transmission point is 520 nm; for No. 21 it is 545 nm). We can only suggest that we found the 450-nm cone much more frequently because our backgrounds were somewhat more selective and of higher light intensity.

The ganglion cell classification scheme used in this study was a very simple

[1] Daw, N. W. Personal communication.

one because of the limitations of our apparatus. Our categorization scheme is similar to one described by Cleland et al. (1973) and Cleland and Levick (1974 *a* and *b*). Therefore, we use their terminology rather than the X, Y, and W terminology originated by Enroth-Cugell and Robson (1966) (X,Y) and elaborated by Stone and Hoffmann (1972) (W). A close association between these two classification schemes has been widely acknowledged (Dubin and Cleland, 1977) but not universally accepted (Shapley and Hochstein, 1975). It was not our intent to elaborate on either scheme but rather to show that our findings were not restricted to one ganglion cell class. The two types of briskly responding cells (presumably X- and Y-cells) could not be distinguished by their cone input. Each of the three photopic systems contributed to ganglion cells of each type. Our sample of sluggishly responding cells (presumably W-cells) is too small to suggest any general conclusions concerning their cone input. None of the four sluggish units we observed had an apparent 450-nm cone input, although in previous work the blue cone system has been associated exclusively with W-cells (Cleland and Levick, 1974 *b*).

A comparison of the structure of the cat retina with that of other mammals, such as the rhesus and owl monkeys, suggests that any functional differences may be quantitative rather than qualitative. For example, the area centralis of the cat resembles the peripheral retina of the rhesus in rod and cone distribution, and the outer plexiform layer of those areas also shows a correspondence by Golgi studies (Boycott and Kolb, 1973).[2] These structural similarities all suggest possible functional analogies.

Although the cat has three functional photopic mechanisms, the rarity of color opponent-type ganglion cells may still leave it behaviorally a dichromat. Behavioral experiments have suggested this to be the case (Brown et al., 1973). However, the owl monkey was shown to be a trichromat only when highly saturated chromatic stimulation was used (Jacobs, 1977). Even slight desaturation made it difficult or impossible for the owl monkey to discriminate yellow from green. This suggests a dichromatism under usual test conditions similar to that of the cat. Until saturated (and large, as suggested by Loop and Bruce [1978]) stimulus lights are used, the possibility of weak trichromatic discrimination by the cat at photopic levels cannot be excluded.

This work was supported, in part, by U.S. Air Force contract F33615-77-C-0209.

*Received for publication 28 November 1978.*

## REFERENCES

BARLOW, H. B., R. FITZHUGH, and S. W. KUFFLER. 1957. Change of organization in the receptive fields of the cat's retina during dark adaptation. *J. Physiol. (Lond.)*. **137**:338–354.

BISHOP, P. O., W. KOZAK, and G. J. VAKKUR. 1962. Some quantitative aspects of the cat's eye: axis and plane of reference, visual field coordinates and optics. *J. Physiol. (Lond.)*. **163**:466–502.

BONAVENTURE, N. 1962. Sensibilité spectrale et vision des couleurs chez le chat. *Psychol. Fr.* **7**: 75–82.

[2] Kolb, H. Personal communication.

BONAVENTURE, N. 1964. La vision chromatique du chat. *Compte Rendu Hebdomadaire des Seánces de l'Academie des Sciences (Paris)*. **259:**2012–2015.

BOYCOTT, B. B., and H. KOLB. 1973. The connections between bipolar cells and photoreceptors in the retina of the domestic cat. *J. Comp. Neurol.* **148:**91–114.

BROWN, J. L., F. D. SHIVELY, R. H. LAMOTTE, and J. A. SECHZER. 1973. Color discrimination in the cat. *J. Comp. Physiol. Psychol.* **84:**(3):534–544.

CICERONE, C. M. 1976. Cones survive rods in the light-damaged eye of the albino rat. *Science (Wash. D. C.)*. **194:**1183–1185.

CLELAND, B. G. and W. R. LEVICK. 1974 *a*. Brisk and sluggish concentrically organized ganglion cells in the cat's retina. *J. Physiol. (Lond.)*. **240:**421–456.

CLELAND, B. G. and W. R. LEVICK. 1974 *b*. Properties of rarely encountered types of ganglion cells in the cat's retina and an overall classification. *J. Physiol. (Lond.)*. **240:**457–492.

CLELAND, B. G., W. R. LEVICK, and K. J. SANDERSON. 1973. Properties of sustained and transient ganglion cells in the cat retina. *J. Physiol. (Lond.)*. **228:**649–680.

CROCKER, R., J. RINGO, M. WOLBARSHT, and H. WAGNER. 1977. Trichromatic cone reception mechanisms in the cat retina. Proc. Int. Union of Physiol. Sci., XXVII Int. Congress, Paris. **13:**153.

DARTNALL, H. J. A. 1953. The interpretation of spectral sensitivity curves. *Br. Med. Bull.* **9:**24–30.

DAW, N. W. and A. L. PEARLMAN. 1969. Cat colour vision: one cone process or several? *J. Physiol. (Lond.)*. **201:**745–764.

DAW, N. W., and A. L. PEARLMAN. 1970. Cat colour vision: evidence for more than one cone process. *J. Physiol. (Lond.)*. **211:**125–137.

DEMONASTERIO, F. M., and P. GOURAS. 1975. Functional properties of ganglion cells of the rhesus monkey retina. *J. Physiol. (Lond.)*. **251:**167–195.

DONNER, K. O., and W. A. H. RUSHTON. 1959. Rod-cone interaction in the frog's retina analyzed by the Stiles-Crawford effect and by dark adaptation. *J. Physiol. (Lond.)*. **149:**303–317.

DUBIN, M. W., and B. G. CLELAND. 1977. Organization of visual inputs to interneurons of lateral geniculate nucleus of the cat. *J. Neurophysiol. (Bethesda)*. **40:**410–427.

ENROTH-CUGELL, C., and J. G. ROBSON. 1966. The contrast sensitivity of retinal ganglion cells of the cat. *J. Physiol. (Lond.)*. **187:**517–552.

FUKUDA, Y., and J. STONE. 1974. Retinal distribution and central projections of X-, Y-, and W-cells of the cat's retina. *J. Neurophysiol. (Bethesda)*. **37:**749–771.

GRANIT, R. 1943. The spectral properties of the visual receptors of the cat. *Acta Physiol. Scand.* **5:** 219–229.

GRANIT, R. 1948. The OFF/ON ratio of the isolated ON-OFF-elements in the mammalian eye. *Br. J. Ophthalmol.* **32:**550–554.

GUNTER, R. 1954. The discrimination between lights of different wavelengths in the cat. *J. Comp. Physiol. Psychol.* **47:**169–172.

GUR, M, and R. PURPLE. 1978. Retinal ganglion cell activity in the ground squirrel under halothane anesthesia. *Vision Res.* **18:**1–14.

HECHT, S. 1937. Rods, cones, and the chemical basis of vision. *Physiol. Rev.* **17:**239–290.

JACOBS, G. H. 1977. Visual capacities of the owl monkey (*Aotus trivirgatus*). I. Spectral sensitivity and color vision. *Vision Res.* **17:**811–820.

KUFFLER, S. W. 1953. Discharge patterns and functional organization or mammalian retina. *J. Neurophysiol. (Bethesda)*. **16:**37–68.

LAMOTTE, R. H., and J. L. BROWN. 1970. Dark adaptation and spectral sensitivity in the cat. *Vision Res.* **10:**703–716.

LENNIE, P., B. G. HERTZ, and C. ENROTH-CUGELL. 1976. Saturation of rod pools in cat. *Vision Res.* **16:**935–940.

LEVICK, W. R. 1972. Another tungsten microelectrode. *Med. Biol. Eng.* **10:**510–515.

LOOP, M. S., and L. L. BRUCE. 1978. Cat color vision: the effect of stimulus size. *Science* (*Wash. D. C.*). **199:**1121–1122.

MELLO, N. K., and N. J. PETERSON. 1964. Behavioral evidence for color discrimination in the cat. *J. Neurophysiol.* (*Bethesda*). **27:**323–333.

MEYER, D. R., and R. A. ANDERSON. 1965. Color discrimination in cats. *In* Color Vision. (A. V. S. de Reuck and J. Knight, editors. Little Brown & Co., Boston. 325–344.

MEYER, D. R., R. C. MILES, and P. RATOOSH. 1954. Absence of color vision in cat. *J. Neurophysiol.* (*Bethesda*). **17:**289–294.

MICHAEL, C. R. 1968. Receptive fields of single optic nerve fibers in a mammal with an all-cone retina. III. Opponent color units. *J. Neurophysiol.* (*Bethesda*). **31:**268–282.

PEARLMAN, A. L., and N. W. DAW. 1970. Opponent color cells in the cat lateral geniculate nucleus. *Science* (*Wash. D. C.*). **167:**84–86.

RINGO, J., M. L. WOLBARSHT, H. G. WAGNER, R. CROCKER, and F. AMTHOR. 1977. Trichromatic vision in the cat. *Science* (*Wash. D. C.*). **198:**753–755.

RODIECK, R. W., and R. W. FORD. 1969. The cat local electroretinogram to incremental stimuli. *Vision Res.* **9:**1–24.

SECHZER, J. A., and J. L. BROWN. 1964. Color discrimination in the cat. *Science* (*Wash. D. C.*). **144:**427–429.

SHAPLEY, R., and S. HOCHSTEIN. 1975. Visual spatial summation in two classes of geniculate cells. *Nature*(*Lond.*).**256:**411–413.

STONE, J., and K. P. HOFFMANN. 1972. Very slow-conduction ganglion cells in the cat's retina: a major new functional type? *Brain Res.* **43:**610–616.

TONG, L. 1977. Rod and cone inputs to color coding and contrast sensitive ganglion cells of the Mexican ground squirrel. Annual Meeting of the Association for Research in Vision and Ophthalmology, Sarasota, Florida, April, 1977. 62. (Abstr.).

WAGNER, H. G., E. F. MACNICHOL, JR., and M. L. WOLBARSHT. 1960. The response properties of single ganglion cells in the goldfish retina. *J. Gen. Physiol.* **43:**(Suppl.:45–60.

WOLBARSHT, M. L., and B. S. YAMANASHI. 1975. Chromophore-protein linkage and the bathochromic shift in visual pigments. Annual Meeting of the Association for Research in Vision and Opthalmology, Sarasota, Florida, April, 1975. 72. (Abstr.).

WOLBARSHT, M. L., and B. S. YAMANASHI. 1977. Intensity sharing, upper and lower limit and genetic dependence of visual pigment absorption spectra. *Biophys. J.* **17**(2, Pt.2):17*a*. (Abstr.).